Electron transport properties of a strained Si layer on a relaxed $Si_{1-x}Ge_x$ substrate by Monte Carlo simulation

H. Miyata,[a] Toshishige Yamada, and D. K. Ferry
Center for Solid State Electronics Research, Arizona State University, Tempe, Arizona 85287-6206

(Received 30 December 1992; accepted for publication 24 March 1993)

The in-plane transport properties of a strained (100) Si layer on a relaxed $Si_{1-x}Ge_x$ substrate are studied with an ensemble Monte Carlo technique. Similar velocity (-field) characteristics are found for strained Si with any valley splitting energy $\Delta E \geqslant 0.1$ eV. These phonon-limited electron mobilities reach 4000 cm^2/V s at 300 K, and 23 000 cm^2/V s at 77 K. There is only a slight increase in the saturation velocity at both temperatures. However, a significant overshoot peak transient velocity is found to depend upon ΔE, and for $\Delta E = 0.4$ eV, reaches 4.1×10^7 cm/s at 300 K, and 5.2×10^7 cm/s at 77 K.

Recent developments in epitaxial growth techniques of $Si/Si_{1-x}Ge_x$ heterostructures has allowed so-called band-gap engineering in this material system. This is reflected in the significant amount of research in this field. In particular, extremely high mobility in an *n*-type modulation doped $Si/Si_{1-x}Ge_x$ heterostructure has been reported, which typically is 1600 cm^2/V s at 300 K and 96 000 cm^2/V s at 4.2 K,[1] or 1500 cm^2/V s at 300 K and 9500 cm^2/V s at 77 K.[2] Peak mobilities of 175 000 cm^2/V s have been achieved at a low temperature.[3] Stimulated by these mobility measurements, a high-transconductance *n*-type $Si/Si_{1-x}Ge_x$ modulation-doped field-effect transistor has been created and exhibits 600 mS/mm at 77 K with a gate length of 0.25 μm.[2] In these latter experiments, a two-dimensional electron gas was realized in a strained Si (100) layer grown on a relaxed $Si_{1-x}Ge_x$ (100) substrate, where the Si layer acts as a potential well and the $Si_{1-x}Ge_x$ substrate acts as a potential barrier, so that a type II superlattice is formed.[4] Once the heterojunction is formed, the strain at the interface causes the sixfold degenerate valleys of Si to split into two groups: two lowered valleys that exhibit a longitudinal mass axis normal to the heterointerface, and four raised valleys that have the longitudinal mass axis parallel to the interface.[4] The conduction band formed by these lowered valleys is now lower than that of $Si_{1-x}Ge_x$ and the band alignment across the heterojunction causes a potential barrier for the electrons which keeps them in the Si layer.

The splitting energy between lowered and raised valleys, ΔE, is empirically represented by $0.6x$ eV, where x is the Ge fraction in the $Si_{1-x}Ge_x$ substrate.[4] The choice $x=0.5$ gives a valley splitting energy as large as 0.3 eV, which is one order of magnitude larger than the thermal energy, even at room temperature. This wide splitting is expected to suppress the intervalley phonon scattering of electrons from lower valleys to upper valleys, and effectively reduces the intervalley phonon scattering rate compared with that of unstrained Si. In the lowered valleys, electrons show the smaller transverse mass in the transport parallel to the interface. This is considered to be the main mechanism for the high mobility and the high transconductance in the devices above.[2] The strain also causes a change in the band-gap E_g, and it is empirically given by $E_g(x) = 1.11 - 0.4x$ eV.[4] This affects the impact ionization and may change the high field transport properties as well. The reduction of band gap is also responsible for a change in the number of electrons in the channel, and may influence the device performance.

We have adopted an ensemble Monte Carlo technique to study the transport properties of a strained Si layer assumed to be grown on a relaxed $Si_{1-x}Ge_x$ substrate. The effect of strain is included only in the band structure as the valley splitting energy ΔE. (In a modulation-doped heterostructure, quantization in the channel adds to the valley splitting,[5] so that we use this simple parameter to characterize the layer.) The effective masses of an electron are assumed to be unchanged[6] and the coupling constants for the various scattering modes are also assumed to be the same. The two-dimensional nature of the scattering in the quantized layer is neglected, since we treat high-field properties. In order to model the smaller transverse-mass transport properly, the explicit inclusion of the longitudinal and transverse masses is important and this is done in the program using the Herring–Vogt transformation[7] with a three-valley model: lowered valley pair 1 is in the (100) direction, raised valley pair 2 is in the (010) direction, and raised valley pair 3 is in the (001) direction, with the electric field in the (001) direction. We use zeroth order *f*- and *g*-phonons and first order *f*- and *g*-phonons for intervalley scattering[8] as well as acoustic phonons. A usual set of coupling constants for phonon modes is adopted, which recovers the measured velocity-field characteristics of unstrained Si reported in Ref. 9 for $x=0$. Impact ionization is also included for the study of higher fields with a soft ionization model by Ridley,[10] which shows a quadratic energy dependence of the scattering rate. The ionization threshold energy E_{th} of strained Si is assumed to be $E_{th}(x) = 1.18E_g(x)/E_g(0)$. When the ionization occurs, a generated electron-hole pair is discarded in the simulation and the original electron loses kinetic energy equal to $E_g(x)$. Nonparabolicity is included using the function $E_g(x)$, and therefore its strength is dependent on x. Although we do not discuss the ionization properties here, their inclusion does affect the observed velocity at the highest fields.

Figure 1 shows the field-velocity characteristics (a) at

[a]Permanent address: Fujitsu Limited, Kawasaki, Japan.

 0003-6951/93/212661-03$06.00

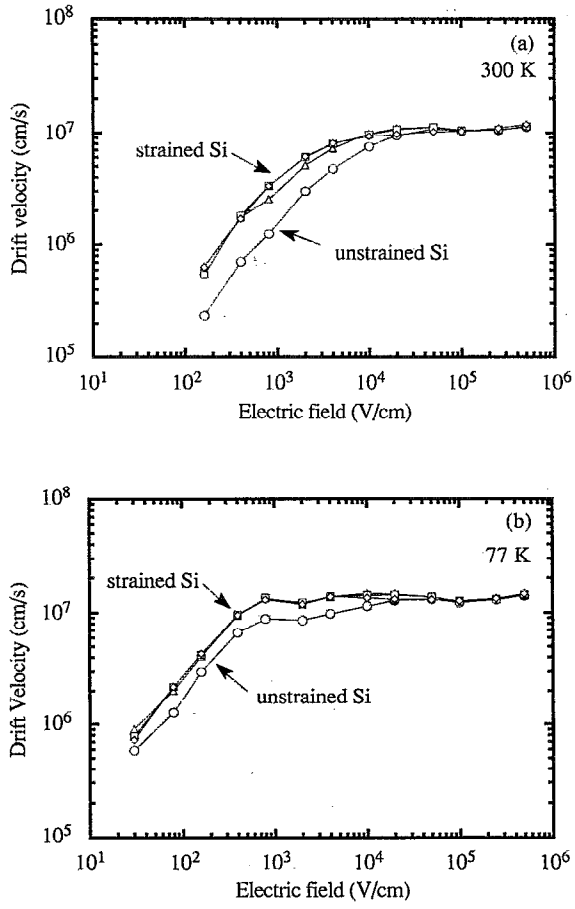

FIG. 1. Velocity-field characteristics of an electron in a strained Si layer for various valley splitting values ΔE, where unstrained Si corresponds to $\Delta E=0$: (a) 300 K and (b) 77 K. The symbol corresponding to each value of ΔE is consistent throughout this letter: ○ for $\Delta E=0$, △ for $\Delta E=0.1$ eV, □ for $\Delta E=0.2$ eV, and ◇ for $\Delta E=0.4$ eV.

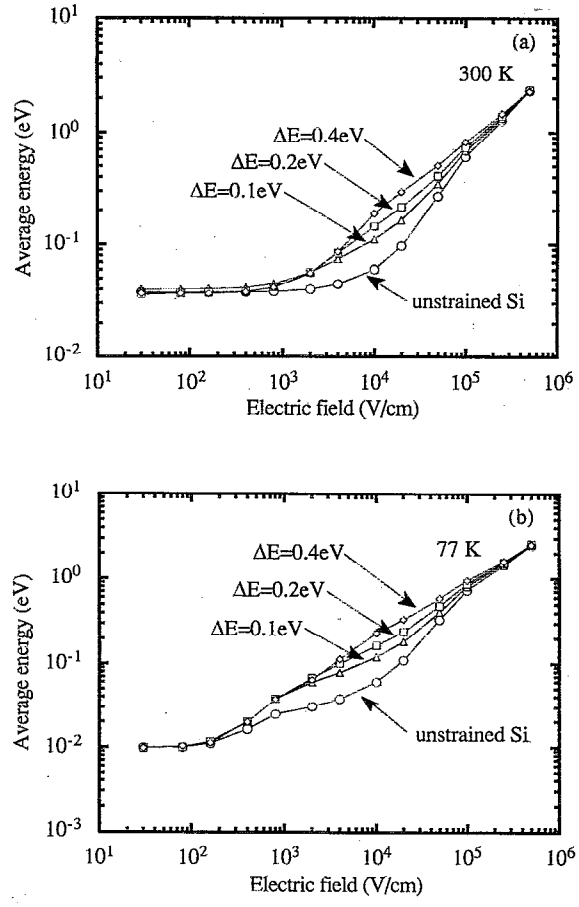

FIG. 2. Energy-field characteristics of an electron in a strained Si layer for various valley splitting values ΔE: (a) 300 K and (b) 77 K.

300 K and (b) 77 K for several valley splitting values $\Delta E=0$, 0.1, 0.2, and 0.4 eV, where "unstrained Si" indicates the characteristics of $\Delta E=0$. The characteristics do not show a significant difference for strained Si with $\Delta E \geq 0.1$ eV, so we can categorize unstrained and strained Si. The mobility for strained Si is almost triple in low field, 4000 cm^2/V s, compared with that of unstrained Si, 1500 cm^2/V s, due to the smaller transverse-mass transport. In fields larger than 20 kV/cm, all curves approach one another and have a similar saturation velocity $\sim 1.0\times 10^7$ cm/s at 300 K, although strained Si tends to show a higher value. The mobility is higher at 77 K, 17 000 cm^2/V s for unstrained Si, and 23 000 cm^2/V s for strained Si, respectively, and the saturation velocity is reached for fields larger than ~ 5 keV/cm. Again, there is no significant difference between them, although strained Si tends to show a slightly higher value. The saturation velocity is estimated to be $\sim 1.3\times 10^7$ cm/s at 77 K.

Figure 2 shows the average electron energy (a) at 300 K and (b) 77 K as a function of the electric field. The energy origin is chosen at the bottom of the lowered valleys (valley pair 1 in the present model), and the average of the sum of kinetic energy and potential energy (0 in the lower valley and ΔE in the upper valleys) is plotted. Energy at thermal equilibrium is $3k_BT/2=39$ meV at 300 K and increases monotonically with the field. The energy has a clear dependence on ΔE, although this is lost in fields larger than 100 kV/cm. In higher fields, electrons have an energy larger than ΔE so there is no significant difference for different ΔE's. It has to be noted that the impact ionization is more important as ΔE increases, since the band gap and therefore the threshold decrease with ΔE. The energy-field characteristics at 77 K are shown in Fig. 2(b). Comparing it with the same plot at 300 K, the electron energy is smaller up to a field 10 kV/cm, and then the order reverses in higher fields, which provides the basis for a larger mobility at 77 K.

As expected, the population equilibriates among the valleys for high fields (and high energies). The electron velocity is markedly faster when electrons are mostly in the lower valleys, in which case intervalley scattering from the lower valleys to the upper valleys is suppressed and the smaller transverse-mass transport is realized. The occupation in the lowest valleys for $\Delta E=0.1$ eV is around 90% even at 300 K, due to low thermal excitation of carriers to the upper valleys. Unstrained Si has an ideal value of 33% over most of the range of the fields, unless an anisotropic electron occupation in the valleys occurs during the transport.

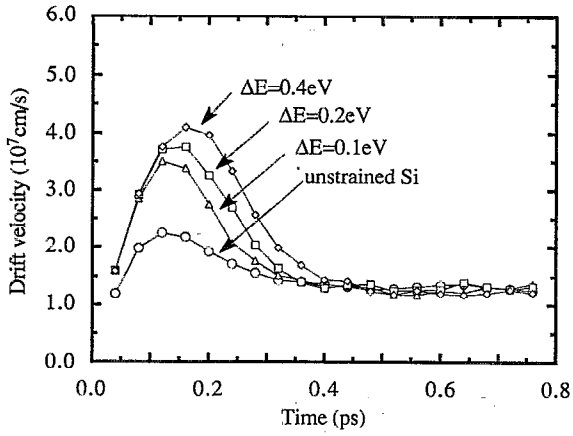

FIG. 3. Transient overshoot velocity with a sudden application of the field 50 kV/cm at 300 K for various valley splitting values ΔE.

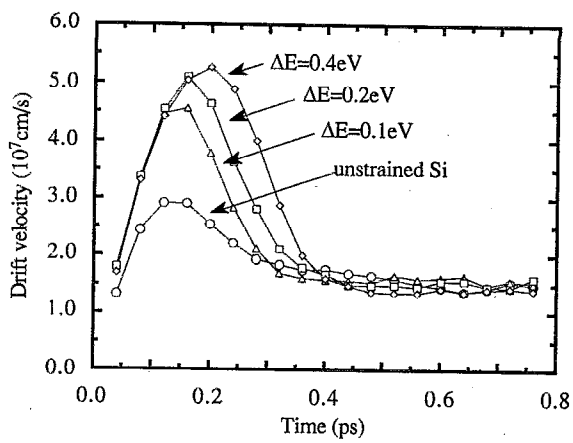

FIG. 4. Transient overshoot velocity with a sudden application of the field 50 kV/cm at 77 K for various valley splitting values ΔE.

Figure 3 shows the transient change of the drift velocity when an electric field of 50 kV/cm is applied suddenly at time $t=0$. The velocity shows a significant overshoot, which is larger for larger ΔE. Around $t=0.3$ to 0.35 ps, the velocity reaches its steady-state value. The peak velocity for $\Delta E=0.4$ eV is 4.1×10^7 cm/s and the overshoot lasts for 0.35 ps. Their product is ~0.1 μm, and this gives an estimation for the device size for which the electrons run from source to drain without reaching the steady-state velocity. This length is the same order of magnitude as the gate length of 0.25 μm in the reported experiment,[2] and their measured high transconductance can be attributed to this overshoot effect, which is more enhanced at 77 K as shown below.

At 77 K, almost 100% of electrons populate the lower valleys, even for $\Delta E=0.1$ eV in low fields. Comparing this with the counterpart at 300 K, there is no significant difference in the fields where the occupation begins to decrease. Figure 4 shows the transient change of the drift velocity at 77 K when an electric field 50 kV/cm is suddenly switched on at $t=0$. The overshoot peak velocity increases again with ΔE, and for $\Delta E=0.4$ eV, it is now 5.2×10^7 cm/s and the transient behavior lasts for 0.4 ps, so that the product is larger (~0.2 μm). The effect of the overshoot is therefore enhanced compared with that at 300 K, and compares well with the effects in the device of Ref. 2.

In summary, we have concluded the transport properties of a $Si/Si_{1-x}Ge_x$ system with an ensemble Monte Carlo technique. Since the strain at the heterointerface releases the degeneracy of the sixfold valleys in unstrained Si, electrons prefer to stay in the lowered valley normal to the interface, which reduces the intervalley scattering and transport is characterized by the smaller transverse mass. The velocity shows similar characteristics for strained Si for $\Delta E\geqslant0.1$ eV, although the electron energy increases with ΔE. The electron mobility for strained Si is estimated to be 4000 cm^2/V s at 300 K, and 23 000 cm^2/V s at 77 K, respectively. There is a slight increase in the saturation velocity compared to that of unstrained Si, at both 300 and 77 K. The overshoot peak velocity with a sudden application of the field 50 kV/cm is larger for larger ΔE, and for $\Delta E=0.4$ eV, it is 4.1×10^7 cm/s at 300 K and 5.2×10^7 cm/s at 77 K, which suggests great potential for future electron device applications.

This work was supported in part by the Office of Naval Research.

[1] Y. J. Mii, Y. H. Xie, E. A. Fitzgerald, D. Monroe, F. A. Thiel, and E. B. Weir, Appl. Phys. Lett. **59**, 1611 (1991).
[2] K. Ismail, B. S. Meyerson, S. Rishton, J. Chu, S. Nelson, and J. Nocera, IEEE Trans. Electron Device Lett. **13**, 229 (1992).
[3] D. Többen, F. Schäffler, A. Zrenner, and G. Abstreiter, Phys. Rev. B. **46**, 4344 (1992).
[4] G. Abstreiter, H. Brugger, T. Wolf, H. Jorke, and H. J. Herog, Phys. Rev. Lett. **54**, 2441 (1985); R. People, IEEE J. Quantum Electron. **22**, 1696 (1985).
[5] T. Ando, A. B. Fowler, and F. Stern, Rev. Mod. Phys. **54**, 437 (1982).
[6] M. M. Rieger, Diplomat Thesis (Prof. Vogl), Technical University Munich, 1991 (unpublished).
[7] C. Jacoboni and R. Reggiani, Rev. Mod. Phys. **55**, 645 (1983).
[8] D. K. Ferry, *Semiconductors* (Macmillan, New York, 1991).
[9] S. M. Sze, *Physics of Semiconductor Devices* (Wiley, New York, 1981).
[10] B. K. Ridley, Semicond. Sci. Technol. **2**, 116 (1987).